Journal Name

ARTICLE

α-Oxidative Decarboxylation of Fatty Acids Catalysed by Cytochrome P450 Peroxygenases Yielding Shorter-Alkyl-Chain Fatty Acids

Received 00th January 20xx,
Accepted 00th January 20xx

DOI: 10.1039/x0xx00000x

www.rsc.org/

Hiroki Onoda[a], Osami Shoji*[a,b], Kazuto Suzuki[a], Hiroshi Sugimoto[b,c], Yoshitsugu Shiro[d], and Yoshihito Watanabe*[e].

Cytochrome P450 peroxygenases belonging to the CYP152 family catalyse the oxidation of fatty acids using H_2O_2. CYP152N1 isolated from *Exiguobacterium* sp. AT1b exclusively catalyses the α-selective hydroxylation of myristic acid under physiological H_2O_2 concentration. However, a series of shorter alkyl-chain fatty acids such as tridecanoic acid were produced from myristic acid by increasing the concentration of H_2O_2 (1-10 mM). The yield of tridecanoic acid from myristic acid reached 17%.^{18}O-labeled oxidant study suggested that CYP152N1 catalysed the overoxidation of α-hydroxymyristic acid to form α-ketomyristic acid, which in turn spontaneously decomposed by H_2O_2 to yield tridecanoic acid. Crystal structure analysis of CYP152N1 revealed high similarity to other CYP152 family enzymes, such as CYP152A1 and CYP152B1. MD simulations of α-hydroxy myristic acid accomodating in CYP152N1 proposed a possible pre-oxidation-conformation of α-hydroxy myristic acid for decarboxylation reaction.

Introduction

Cytochrome P450s (CYPs or P450s) are monooxygenases found in a plethora of animals, plants and microorganisms[1]. P450s catalyse the oxidation of a variety of organic compounds related to biological, pharmaceutical, and medicinal chemistry. Most P450s utilise molecular oxygen for monooxygenation reactions[2], in which electrons are provided by NAD(P)H to generate the haem active oxygen species (Compound I). In 1996, Matsunaga and co-workers reported a peroxygenase activity of Cytochrome $P450_{SPα}$ (CYP152B1) isolated from *Sphingomonas paucimobilis*[3, 4], which catalyses the α-selective hydroxylation of long-chain fatty acids[5]. CYP152B1 exclusively oxidizes fatty acids[6]. Moreover, the K_m for H_2O_2 of the peroxygenation catalysed by CYP152B1 was sufficiently low (72 μM)[7]. Accordingly, CYP152B1 was classified as a fatty acid peroxygenase (EC 1.11.2.4). The crystal structure of a fatty acid bound-form of CYP152B1 (PDB: 3AWM)[8] showed the carboxylate moiety of the fatty acid interacting with Arg241 located at the distal side of the haem prosthetic group. This arginine is highly conserved in other fatty acid peroxygenases, such as $P450_{BSβ}$ (CYP152A1) isolated from *Bacillus subtilis*[9] and $P450_{CLA}$ (CYP152A2) isolated from *Clostridium acetobutylicum*[10]. Both CYP152A1 and CYP152A2 catalyse α- and β-hydroxylation of fatty acids[11, 12]. The K_m of H_2O_2 for fatty acid hydroxylation by CYP152A1 was estimated to be 21 μM[13]. Based on crystal structure analysis of CYP152A1, a reaction mechanism for the formation of the active oxygen species (Compound I) was proposed, wherein the carboxylate group of the fatty acid interacting with the distal arginine serves as an acid-base catalyst for the activation of hydrogen peroxide (Scheme 1A)[14]. In fact, mutation of the distal arginine to alanine (R242A) decreased both the affinity for hydrogen peroxide (K_m = 4.4 mM) and the catalytic activity (k_{cat} = 0.83 min^{-1})[13]. Recently,

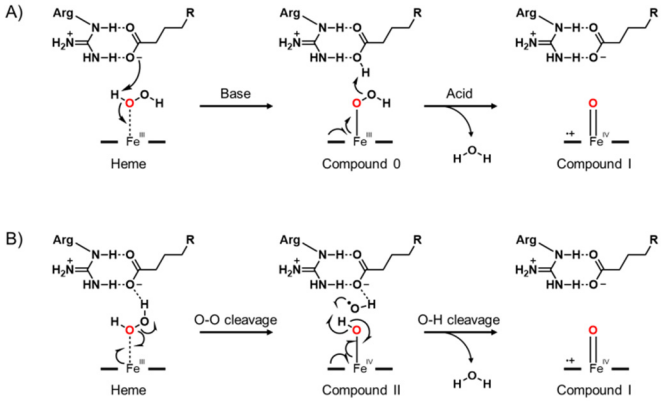

Scheme 1 Compound I formation mechanisms of CYP152 family enzymes

[a] Department of Chemistry, Graduate School of Science, Nagoya University, Furo-cho, Chikusa-ku, Nagoya 464-0802, Japan. Email: shoji.osami@a.mbox.nagoya-u.ac.jp
[b] Core Research for Evolutional Science and Technology (CREST), Japan Science and Technology Agency, 5 Sanban-cho, Chiyoda-ku, Tokyo, 102-0075, Japan
[c] RIKEN SPring-8 Center, 1-1-1 Kouto, Sayo-cho, Hyogo 679-5148, Japan
[d] Graduate School of Life Science, University of Hyogo, 3-2-1 Kouto, Kamigori, Ako, Hyogo 678-1297, Japan
[e] Resarch Center for Materials Science, Nagoya University, Furo-cho, Chikusa-ku, Nagoya 464-0802, Japan. Email: p47297a@nucc.cc.nagoya-u.ac.jp
† Footnotes relating to the title and/or authors should appear here.
Electronic Supplementary Information (ESI) available: [Materials section, Amino acid sequence of CYP152 family enzymes, and Supplementary figures (Fig. S1-14)]. See DOI: 10.1039/x0xx00000x

Quantum Mechanical/Molecular Mechanical (QM/MM) and Molecular Dynamics (MD) studies suggested another mechanism[15] (Scheme 1B), wherein the carboxylate group of the fatty acid plays an important role in orienting the hydroxyl radical (HO·) toward Compound II. The interaction of the carboxylate moiety with the distal arginine is critical for active oxygen species formation in both mechanisms. Previous research on chemical rescue by acetate-anions enabling non-native substrates hydroxylation lend support to a carboxylate-dependent mechanism[16].

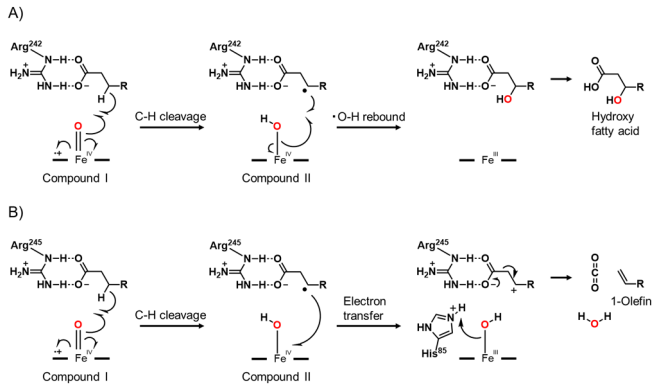

Scheme 2 Possible reaction mechanisms of fatty acid preoxygenation reactions catalysed by A) CYP152A1 and B) CYP152L1

Although CYP152 family enzymes have been considered to solely play a role in fatty acid hydroxylation reactions, this paradigm came under scrutiny in 2011 with the discovery of $OleT_{JE}$ (CYP152L1) isolated from *Jeotgalicoccus* sp. ATCC 8456, which catalyses terminal olefin biosynthesis from fatty acids[17, 18]. The terminal olefin is produced via a fatty acid decarboxylation reaction[19, 20] (Scheme 2B), which can be initiated by C-H abstraction[21] in the same manner as fatty acid hydroxylation by CYP152A1 (scheme 2A). In addition, it was reported that CYP152A1 also produced a small amount of terminal olefin[17], while CYP152A2 does not produce any terminal olefin[22]. Recently, it was reported that three CYP152 family enzymes, such as CYP-MP (CYP152P1) isolated from *Methylobacterium populi*, CYP-Aa162 (CYP152A8) isolated from *Alicyclobacillus acidocaldarius*, and CYP-Sm46 (CYP152L2) isolated from *Staphylococcus massiliensis*, can also produce terminal olefins[23, 24]. These results clearly show that CYP152 family enzymes possess potential to perform reactions other than fatty acid hydroxylation, encouraging us to explore other CYP152 family enzymes.

Herein we report that the α-oxidative decarboxylation reaction of fatty acids can also be catalysed by CYP152N1 ($P450_{Exα}$) isolated from *Exiguobacterium* sp. AT1b[25], which was obtained from the hot springs of Yellowstone National Park. Shorter-alkyl-chain fatty acids including tridecanoic acid were produced from myristic acid, upon increase of the hydrogen peroxide concentration. The amino-acid sequence of $P450_{Exα}$ possesses a 44% sequence identity to CYP152A1, leading to its classification as CYP152N1. Crystal structure analysis showed that CYP152N1 had the distal arginine which was critical for fatty acids binding. We investigated a possible reaction mechanism for α-oxidative decarboxylation by using an experimental approach employing ^{18}O-labelled hydrogen peroxide as an oxygen source in combination with MD simulations based on the crystal structure of fatty acid-bound form of CYP152N1.

Results and Discussion

UV-vis spectra and myristic acid oxidation

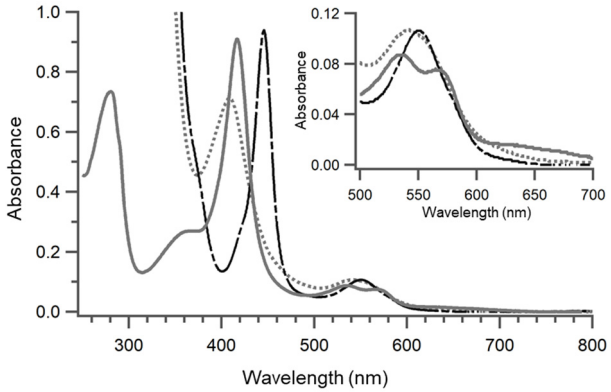

Fig. 1 UV-vis spectra of CYP152N1 (6.2 μM) of ferric form (solid line), ferrous form (dotted line), CO binding ferrous form (chain line).

The UV-VIS spectrum of purified CYP152N1 (Fig. S1) showed a Soret band absorption peak at 417 nm and two Q-band absorption peaks at 542 nm and 565 nm (Fig. 1 solid line), indicative of the typical low spin ferric state of P450s. The absorption of dithionite-reduced ferrous-CO adducts was observed at 444 nm (Fig. 1 chain line), indicative of thiolate ligation to the haem iron. Upon addition of myristic acid or palmitic acid to ferric CYP152N1, the Soret band absorption peak slightly shifted to a shorter wavelength (Fig. S2). Type I shifts are caused by displacement of water from the haem resulting in a spin state change of the haem Iron from low to high spin, indicative of positive substrate binding. Dissociation constants (K_d) of palmitic acid and myristic acid were estimated to be 47 μM and 6.5 μM, respectively (Fig. S3).

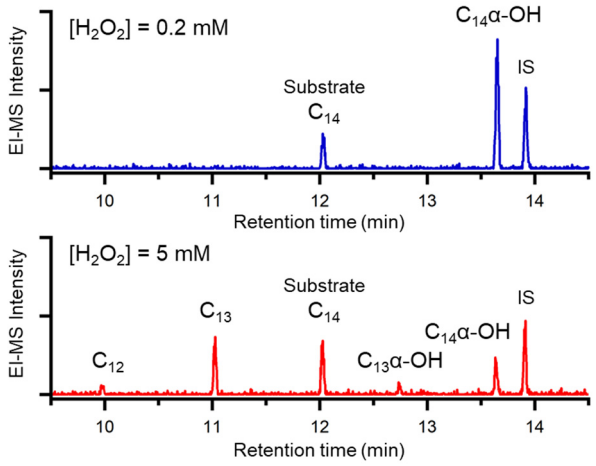

Fig. 2 GC-MS chart (MIC m/z = 117, 147) of myristic acid oxidation in the presence of 200 μM or 5 mM H_2O_2. Retention time of TMS derivatives: C_{12} (10.0 min), C_{13} (11.0 min), C_{14} (12.0 min), C_{13}α-OH (12.7 min), C_{14}α-OH (13.7 min), C_{14}β-OH (13.8 min) IS (Internal standard, 13.9 min).

Hydroxylation of myristic acid was examined using CYP152N1 by changing the concentration of myristic acid as well as H_2O_2. The GC-MS chart showed the peak of α-hydroxy myristic acid in the presence of 200 μM hydrogen peroxide (Fig. 2A). The appreciable peaks corresponding to β-hydroxy myristic acid or 1-tridecene was not detected. The configuration of α-hydroxy myristic acid was confirmed by HPLC equipped with a chiral column (Fig. S4) to be dominantly (*S*)-form (91%ee). The regio- and stereo-selectivity of myristic acid hydroxylation were similar to those of CYP152B1[6, 8]. Michaelis-Menten kinetic analysis (Fig. S5) revealed that the k_{cat} reached 1900 ± 130 min^{-1}, which is higher than that of both CYP152A1 (1400 ± 180 min^{-1}) and CYP152B1 (1300 ± 20 min^{-1}). The K_m of CYP152N1 for myristic acid (130 ± 20 μM) was higher than that of CYP152A1 (66 ± 20 μM) and CYP152B1 (43 ± 2 μM)[8].

Interestingly, tridecanoic acid could be detected when the concentration of H_2O_2 was raised to 5 mM. GC-MS analysis allowed the detection of peaks corresponding to tridecanoic acid, lauric acid, and α-hydroxy tridecanoic acid (Fig. 2B, S6). The maximum yield of tridecanoic acid produced from myristic acid in a one-minute oxidation reaction was 17% using 10 mM H_2O_2 (Fig. 3). We also found that myristic acid was primarily converted to decanoic acid (C_{10}) by 20 minutes reaction using CYP152N1 (Fig. S7).

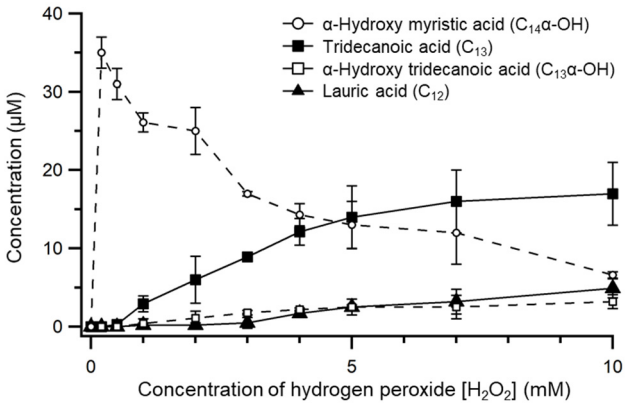

Fig. 3 Fatty acids concentration of the product mixture after oxidation of myristic acid catalysed by CYP152N1

The yield of tridecanoic acid was enhanced by increasing the concentration of hydrogen peroxide accompanied by a decrease in α-hydroxy myristic acid (Fig. 3). These results implied that tridecanoic acid was produced by oxidation of α-hydroxy myristic acid. α-Hydroxy myristic acid would have a chance to be further oxidised, because α-hydroxy myristic acid also possesses the carboxylate group which accelerates the formation of Compound I of CYP152N1 using H_2O_2. In fact, tridecanoic acid was produced when α-hydroxy myristic acid was used as a starting substrate (Fig. S8). α-Hydroxy myristic acid should be further oxidised to give α-keto myristic acid, whilst the α-keto fatty acid intermediate was not detected by GC-MS. It was reported that various α-keto acids such as pyruvic acid[26] and 4-methyl-2-oxopentanoic acid[27] were spontaneously decarboxylated by H_2O_2 under neutral or basic conditions (Scheme 3)[28, 29]. We presume that α-keto myristic acid was consumed by H_2O_2 via non-enzymatic decarboxylation to yield tridecanoic acid.

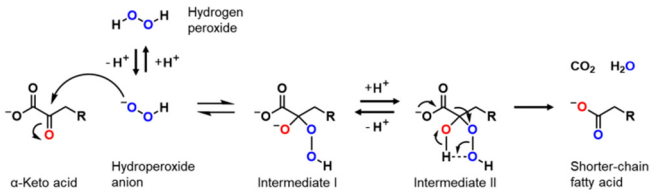

Scheme 3 Reported catalytic reaction mechanism of α-keto decarboxylation.

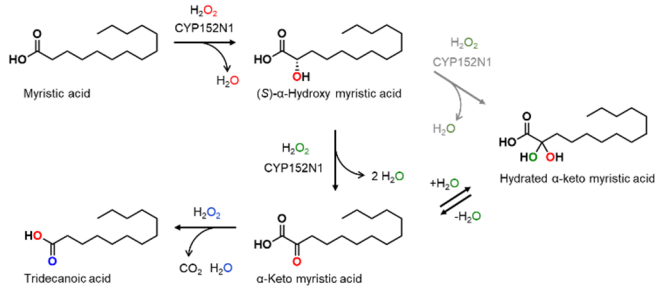

Scheme 4 Proposed reaction scheme of tridecanoic acid formation.

A possible reaction scheme of tridecanoic acid formation reactions is shown in Scheme 4. Herein, the carboxylate of myristic acid is eliminated as carbon dioxide. To confirm the elimination of carboxylate, the oxidation of myristic acid by CYP152N1 was carried out using ^{18}O-labelled hydrogen peroxide ($H_2{}^{18}O_2$). Tridecanoic acid produced from myristic acid and $H_2{}^{18}O_2$ contained two ^{18}O-labelled atoms as the major product (Fig. S9A). This result indicated $C^{16}O_2$ was released from myristic acid after stepwise oxidation. Upon the oxidation of α-hydroxy myristic acid ($C_{14}α$-^{16}OH), mono-^{18}O-labelled tridecanoic acid was the main product (Fig S9B). These consistent results suggested that one oxygen atom originated from the hydroxyl group of α-hydroxy myristic acid was introduced to the product. The fact indicated that most of α-keto acids were produced without going through the hydrated-α-keto acid, which could be produced by the (*R*)-α-hydroxylation of (*S*)-α-hydroxy myristic acid, while it was reported that α-keto acids had chance to hydrated by water[30]. A small amount of mono-^{18}O-labelled tridecanoic acid was produced in the presence of ^{18}O-labelled water (Figure S10), although there was no ^{18}O-labelled myristic acid present. These results indicate that the α-keto acid intermediate can be partially hydrated by water, offering a plausible reason of α-keto acid formation in the α-oxidative decarboxylation of myristic acid.

Crystal structure analysis and MD simulation analysis

To evaluate the enzymatically catalysed reaction mechanism of α-keto acid formation reaction, we performed the structure analysis of substrate-bound form of CYP152N1. CYP152N1 was crystallised by sitting drop vapour diffusion method. The crystal structure of CYP152N1 was solved at 2.3 Å resolution (Fig. 4A, PDB: 5YHJ). The overall structure of CYP152N1 possessed a typical "P450 fold"[31, 32] with a cysteine (Cys359) thiolate coordinated to the haem *b* cofactor (Fig. S11). A long

electron density assignable to myristic acid was observed (Fig. S12). The carboxylate of myristic acid interacts with Arg239 at the distal side of haem (Fig. 4B). The distance between the haem iron and α-carbon atom of myristic acid was 5.2 Å, which is shorter than that of the β-carbon atom at 6.6 Å. This observation is consistent with the α-selective hydroxylation of myristic acid obtained in experiments. It is noteworthy to mention here that Phe286 was observed at the corresponding position to Phe288 in CYP152B1, which plays a critical role in governing α-selective hydroxylation[8, 33].

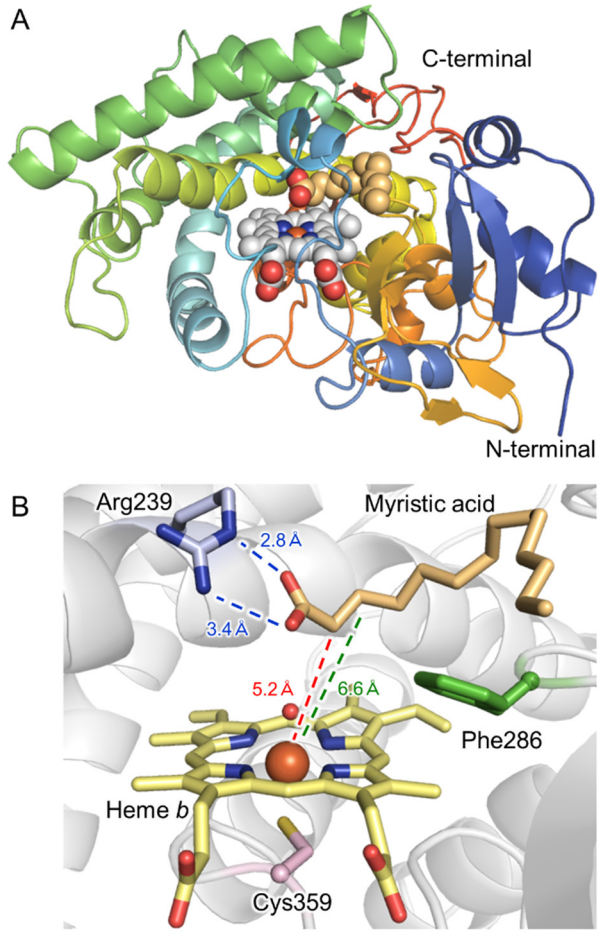

Fig. 4 Whole structure (A) and active site structure (B) of myristic acid bound CYP152N1 (PDB: 5YHJ). Myristic acid, haem *b*, and amino residues are shown as sphere model or stick model. Main chain of CYP152N1 is shown as ribbon model.

For the formation of α-keto myristic acid from α-hydroxy myristic acid, the α-carbon atom of α-hydroxy myristic acid needs to be near the haem iron in the same way to myristic acid. To evaluate the binding of α-hydroxy myristic acid into the active site of CYP152N1, we performed molecular dynamics (MD) simulations of α-hydroxy myristic acid in the CYP152N1 crystal structure. The initial model for α-hydroxy myristic acid was prepared by transforming the pro-(*S*)-hydrogen atom, which is locating at the α-position of myristic acid in the CYP152N1 active site, into a hydroxy group. The oxo atom of Compound I was placed at 1.65 Å perpendicular from the centre of the porphyrin ring. The carboxylate of (*S*)-α-hydroxy myristic acid remained hydrogen bonded to Arg239 throughout the entirety the 100 ns MD simulations (Fig. S13). The α-carbon atom of (*S*)-α-hydroxy myristic acid was closed to heme iron. These results lend further support to the enzymatic oxidation of (*S*)-α-hydroxy myristic acid.

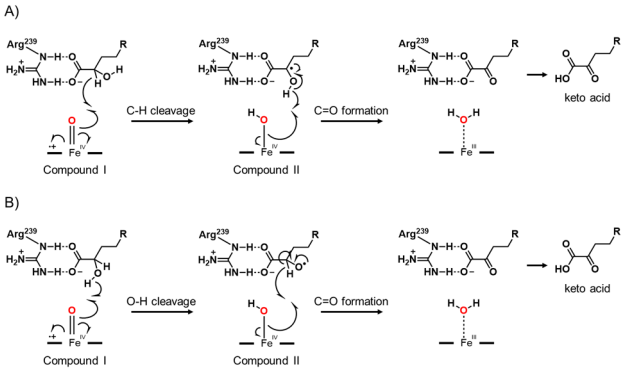

Scheme 5 Possible reaction mechanism of α-keto myristic acid formation.

The possible catalytic reaction mechanisms of α-keto acids formation reaction were shown in Scheme 5. The C-H dissociation (Scheme 5A) and the O-H dissociation (Scheme 5B) were possible to be catalysed by CYP152N1. However, the MD simulation results supported the oxidation of (*S*)-α-hydroxy myristic acid to α-keto myristic acid via the α-O-H cleavage mechanism (Scheme 5B), since the (*R*)-α-hydrogen atom was not shown to access the oxygen atom of Compound I during the simulation time (Fig. 5).

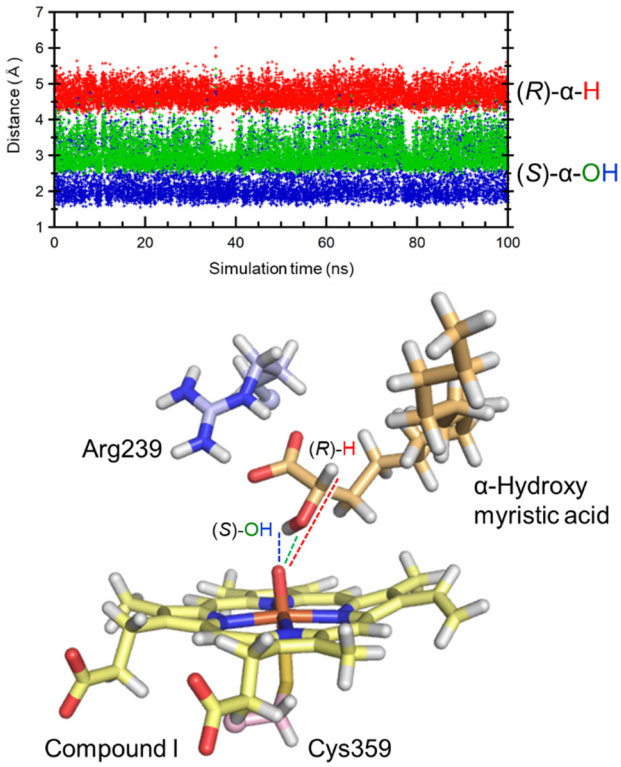

Fig. 5 100ns distribution of distance from oxygen atom of compound I to hydrogen atoms of (*S*)-α-hydroxy myristic acid. The plots of hydrogen atom of hydroxy myristic acid at (*S*)-α-hydroxy group were shown as blue colour. The plots of (*R*)-α-hydrogen atom were shown as red colour. The plots of oxygen atom at (*S*)-α-hydroxy group were shown as green colour.

α-Oxidative Decarboxylation Reaction by Other CYP152s

The α-oxidative decarboxylation reaction under high concentration (1-10 mM) hydrogen peroxide was not reported within 20 years from the discovery of CYP152s. Denning and Faber *et al*. reported the myristic acid oxidation reaction of CYP152L1 and CYP152A2 in the presence of 5 mM hydrogen peroxide[22], however, shorter chain fatty acids such as tridecanoic acid and lauric acid were not detected. Interestingly, CYP152B1, which is an α-selective fatty acid peroxygenase, catalyses the α-oxidative decarboxylation reaction of myristic acid at 5 mM hydrogen peroxide (Fig. 6B). Moreover, CYP152A1 catalyses the α-oxidative decarboxylation reaction in concert with terminal-olefin-productive decarboxylation reaction, α-hydroxylation reaction, and β-hydroxylation (Fig. 6A).

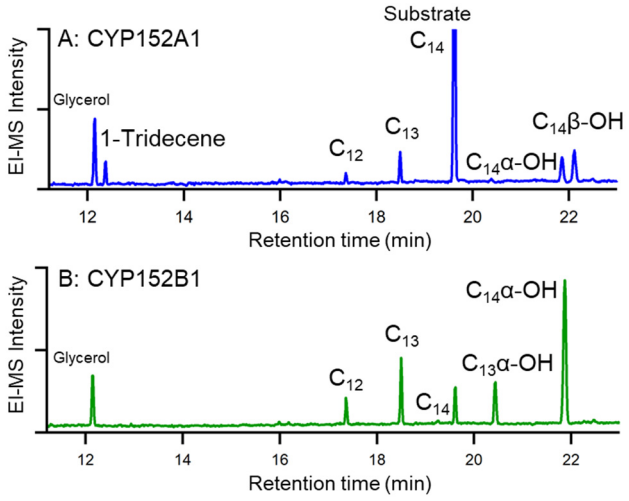

Fig. 6 GC-MS chart of myristic acid (C_{14}) oxidation catalysed by CYP152A1 (A) and CYP152B1 (B) in the presence of 5 mM H_2O_2. The TMS derivatized products were analysed using a Shimadzu GCMS-QP2010 and DB-624 capillary column (30 m × 0.32 mm; Agilent Technologies, Inc., Santa Clara, CA). Retention time: 1-Tridecene (12.4 min), C_{12} (17.4 min), C_{13} (18.5 min), C_{14} (19.6 min), C_{13}α-OH (20.4 min), C_{14}α-OH (21.9 min), C_{14}β-OH (22.1 min).

Conclusions

CYP152N1 catalysed the α-(*S*)-selective hydroxylation of myristic acid in the presence of physiological concentrated hydrogen peroxide. Crystal structure analysis supports the high regio-selectivity of fatty acid oxidation. Following the addition of excess hydrogen peroxide (> 5 mM), CYP152 family enzymes switched to the production of shorter-chain fatty acid such as tridecanoic acid as the main product. This α-oxidative decarboxylation reaction consists of two distinct enzymatic steps; 1) fatty acid α-hydroxylation, 2) α-keto acid formation, followed by a third enzyme independent step; 3) α-keto acid decarboxylation. It was reported that CYP152L1 catalyses the olefin-productive (β-oxidative) decarboxylation reaction of various chain-length fatty acids such as arachidic acid (C_{20}) and butanoic acid (C_4). Although CYP152L1 ($OleT_{JE}$) was regarded as the best enzyme to produce biofuels as alkenes instead of bio-alcohols and bio-diesels, the ideal chain length of biofuels for industry or gasoline are shorter than the produced biologically relevant fatty acids such as stearic acid (C_{18}), palmitic acid (C_{16}), myristic acid (C_{14}), and these unsaturated fatty acids. Further optimization of the reaction conditions is predicted to enable control over both α-oxidative decarboxylation activities and terminal-olefin productive decarboxylation activities of CYP152 to generate ideal biofuels from recyclable biological resources.

Experimental Section

Preparation and Purification of Enzymes

Recombinant CYP152B1 possessing a GST-tag at its N-terminal was expressed in *Escherichia coli* BL21 (DE3) [pGEX-AX2-CYP152B1] and purified by GST affinity chromatography. Recombinant CYP152A1 with a 6×Histidine-tag at its N-terminal was expressed in Escherichia coli M15 [pQE30t-CYP152A1, pREP4] and purified via nickel chelate affinity chromatography. GST-tag and 6×histidine-tag were removed from both P450s by digestion with thrombin, followed by further purification via gel filtration using BioAssist eZ according to a reported procedure[13]. pQE30t-CYP152N1 (Fig. S1A) was designed from pQE30t-CYP152A1 and the synthetic nucleic acid (pBlueScript II SK (+)-CYP152N1) as described in the supporting information. About 18 mg/L of CYP152N1 with 6xHis-tag at N-terminal were expressed in the soluble fraction. CYP152N1 was purified in the same way to CYP152A1[13]. P450s in GB Buffer (100 mM potassium phosphate buffer with 0.3 M potassium chloride and 20% glycerol) were flash frozen in liquid nitrogen and stored at -80°C. The concentration of P450s was calculated from the haem concentration determined via pyridine ferro-hemochrome assay ($\varepsilon_{R,557}$ = 34.7 mM^{-1} cm^{-1})[34, 35].

Measurements

UV-visible spectra were recorded until no further absorbance change occurred using a UV-2600 spectrophotometer (Shimadzu) at 25°C. Spectra of ferric-CYP152N1 were recorded 6.2 μM under 100 mM potassium phosphate buffer with 0.3 M potassium chloride and 20% glycerol. Ferrous-CYP152N1 was prepared by the addition of sodium dithionate to ferric-CYP152N1 solution. Spectra of ferric-CYP152N1 in complex with substrate were recorded following the addition of myristic acid, dissolved in 70% (v/v) EtOH/water solution. The dissociation constant K_d was approximated from the absorbance difference of the substrate free form by fitting with either a dissociation equation.

Hydroxylation of Myristic Acid

The reaction cocktail contained 0.1 M potassium phosphate (pH 7.0), 0-250 μL of Myristic acid (C_{14}), 50 nM of CYP152N1 and 200 μM of H_2O_2 in a total volume of 1 mL. The reaction mixture was incubated at 37°C for 1 min, and thereafter the reaction was quenched with 2 mL of dichloromethane followed by vigorous mixing. After the addition of ω-hydroxy lauric acid (C_{12}ω-OH) as an internal standard, the products were extracted in dichloromethane. For derivatization of the extract, 25 μL of 0.01% (w/v) 9-anthryldiazomethan (ADAM®) acetone solution was added, followed by incubation in the dark at room temperature for 1 hr. Products were quantified by reverse phase HPLC analysis on a Shimadzu SCL-10A_{VP} systems equipped with Inertsil® ODS-3 column according to a reported method[8]. The HPLC analytical conditions were as follows: flow rate 1.0 mL/ min; acetonitrile/water = 99/1; column

temperature, 30°C; extension wavelength, 365 nm, emission wavelength 412 nm; and retention times, C_{12}ω-OH (6.63 min), β-hydroxy myristic acid (C_{14}β-OH, 11.0 min), α-hydroxy myristic acid (C_{14}α-OH, 12.3 min), C_{14} (22.2 min). To determine enantioselectivity of the products, reverse phase HPLC analysis was performed using a Chiralpak AD-RH column installed on a Shimadzu SCL-10A_{VP} systems. The retention time was determined using arsenic samples. The absolute configuration was assigned by the product ratios of the myristic acid hydroxylation catalysed by CYP152A1[13] and CYP152B1[6]. The HPLC analytical conditions were as follows: flow rate 0.9 mL/ min; liner gradient MeOH/water = 85/15 (0-10 min) to 100/0 (100-120 min); column temperature, 40°C; extension wavelength, 365 nm, emission wavelength 412 nm; and retention times, C_{14}α-(*R*)-OH (33 min), C_{14}α-(*S*)-OH (36 min), C_{14}β-(*R*)-OH (50 min), C_{14}β-(*S*)-OH (53 min), C_{14} (57 min).

Oxidation of Myristic Acid under Elevated Concentration of Hydrogen Peroxide

The reaction mixture contained 0.1 M potassium phosphate (pH 7.0), 100 µM of Myristic acid (C_{14}), 1 µM of CYP152N1 and 0.2-5 mM of H_2O_2 in a total volume of 1 mL. The reaction mixture was incubated at 37°C for 1 min, upon which the reaction was quenched with 1 mL of dichloromethane followed by vigorous mixing. At the same time, 5 µL of 1 mM palmitic acid (C_{16}) ethanol solution was added as the internal standard. Reaction products and internal standard were extracted in dichloromethane. For the derivatization of the extract, 25 µL of N,O-bis(trimethylsilyl)trifluoroacetamide (BSTFA) containing 1% (v/v) trimethylchlorosilane (TMCS) was added to 25 µL of dichloromethane extract solution, and the mixture was incubated at room temperature for more than 1 h. The derivatised products were analysed using a Shimadzu GCMS-QP2010 and Rxi™-5ms capillary column (30 m × 0.25 mm; Restek Corp., Bellefonte, PA). The GC/MS analytical condition were as follows: column temperature, 50°C (1 min) to 40°C/min (5 min) to 250°C (8 min); injection temperature, 250°C; interface temperature 280°C; carrier gas, helium; flowrate, 0.9 ml/min; mode, split mode; and split ratio, 1/50. the peaks of C_{14} (12.8 min), C_{14}α-OH (14.4 min), C_{14}β-OH (14.6 min) and C_{13} (11.7 min) C_{12} (10.7 min) were determined by the mass fragment patterns and authentic samples. The peaks of C_{13}α-OH were determined just by the mass fragment patterns because authentic samples were not available. The concentrations of substrate and products were determined by a calibration curve of the ratio of products and internal standard peak area.

^{18}O-Labelled Oxidant Reaction

The reaction mixture contained 0.1 M potassium phosphate (pH 7.0), 100 µM of Myristic acid (C_{14}), 50 nM of CYP152N1 and 5 mM of 90% ^{18}O labelled H_2O_2 in a total volume of 0.5 mL. The reaction mixture was incubated at 37°C for 10 min, whereupon the reaction was quenched by 1 mL of dichloromethane followed by vigorous mixing. At the same time, the products were extracted by with dichloromethane. The method of the GC/MS analyse was described above.

Crystallisation of CYP152N1

The buffer for the purified CYP151N1 solution was exchanged to 50 mM MES buffer (pH 7.0) and 20% (v/v) glycerol. CYP152N1 was concentrated to 16.4 mg/ml by centrifugation using Amicon Ultra filters units (Millipore, Co.). The crustal of CYP152N1 was grown by the sitting-drop vapour diffusion using the reservoir solution 0.1 M Tris hydrochloride pH 8.5, 0.2 M magnesium chloride, 30% polyethylene glycol 4,000 (A2 reagent of Pre-Crystallization Test, Hampton Research). For the sitting-drop, 2 µL of CYP152N1 solution was mixed with 2 µL of the reservoir solution. The crystals of CYP152N1 for diffraction experiment were dialyzed against the cryoprotectant solution containing 25 mM MES 0.05 M Tris hydrochloride, 0.1 M magnesium chloride hexahydrate, 30% w/v polyethylene glycol 4,000 and 10% glycerol for two days.

Data Collection and Refinement

Crystals were flash-cooled in nitrogen gas stream at 100K. X-ray-diffraction data sets were collected at wavelength of 1.0 Å on beam line BL26B1 at RIKEN SPring-8 (Hyogo, Japan) The program HKL2000[36] was used for the integration and scaling of the diffraction data. The initial phase of the CYP152N1 crystal was obtained using MOLREP[37]. The atomic model was refined using REFMAC5[38], phenix.refine[39], and COOT[40]. TLS refinement[41] was performed at the final stage of the refinement by defining 8 separate TLS groups (chain A: 2-88, 89-226, 227-377, 378-412, chain B: 2-88, 89-257, 258-377, 378-412). The resulting models had a final R_{work} of 21.4% and an R_{free} of 24.8% (Table 1).

Table 1 Data collection and refinement statistics

Data collection		Refinement	
Space group	$P4_1$	Resolution	19.75-2.30
Cell dimensions		No. reflections	35736
a b c (Å)	58.96 58.96 238.34	R_{work}/R_{free}	0.2142/0.2478
Resolution	20.00-2.30 (2.38-2.30) *	No. of atoms	
R_{merge}	5.2 (33.0)	Protein	6686
$I/\sigma(I)$	22.0 (5.1)	Ligand	118
$CC^{1/2}$	(0.981)	Water	61
Completeness	99.6 (100)	r.m.s deviations	
Redundancy	6.8 (6.7)	Bond lengths (Å)	0.009
Wilson B (Å)	37.2	Bond angles (°)	1.1

*Values in parentheses are for the highest-resolution shell.; r.m.s.: root mean square

MD Simulation of Myristic Acid and α-Hydroxy Myristic Acid

MD simulations were performed by using Maestro with Desmond/GPU program[42]. The crystal structure of myristic acid binding CYP152N1 was used as an initial template for MD simulations of myristic acid. The template of α-hydroxy myristic acid was prepared by exchanging the (*S*)-α-hydrogen atom with oxygen atom. The water molecules present in the crystal structure were removed. Compound I was modelled from the haem and the oxygen atom of the axial ligand at 1.65 Å above the Fe atom[43, 44] . Hydrogen atoms were prepared by the protein preparation wizard of Maestro. Protons of titratable residue at pH 7.0 were estimated by PROPKA[45, 46]. All side chains of glutamine, asparagine and histidine were not flipped, and all carboxyl groups of glutamic acids and aspartic acids were deprotonated. Histidine 94 was only double-protonated on the aromatic nitrogen atoms. The proton of His208, His256, His363, and His408 were prepared on δ-position, and that of His13, His92, His217, His319, and His357 were prepared on ε-position. The solvent box was prepared by

TIP4P[47], 12 sodium cations were added to neutralise the total change, and ions of 0.15 M sodium chloride were added to reduce the interaction between hydrophilic residues at the protein surface using System builder of Desmond[48]. The R.E.D. III derived atomic partial charge of Compound I and thiolate ligand (Cys 359)[49] were used for our simulations. The protein back bone, Arg239 side chain, and Compound I, except for the hydrogen atoms were restrained by the force constant of 100 kcal (mol Å)$^{-1}$ to prepend braking of the CYP152N1 structure during the simulations. The simulation system was equilibrated using the default protocol of Desmond. After a 5 ns relaxation simulation, a 100 ns MD simulation was performed under following conditions: equilibration of simulation was used isothermal isobaric ensemble (NPT), forcefield was used as OPLS-2005[50], the short-range electrostatic interactions between over 10 Å divided atoms were cut off, long-range electrostatic interactions were computed with Particle Mesh Ewald method, all covalent bonds involving hydrogen atoms were constrained using the SHAKE algorism[51], the thermostat and barostat were used as Nose-Hoover chain[52-54] at 300K and Martyna-Tobias-Kien[55] at 1 atm with relaxation of 1 ps and 2 ps, RESPA integrator[56] was used with Fourier-space electrostatics computed every 6 fs and all remaining interactions computed every 2 fs. The result of MD simulation was analysed by Simulation Event Analysis of Desmond. Before the MD simulation of α -hydroxy myristic acid, we checked the evaluation condition using 100 ns MD simulation of myristic acid in the active site of CYP152N1. The distance distribution between oxygen atom of compound I and hydrogen atoms of myristic acid suggested α-selectivity (98%) and (*S*)-selectivity (84%ee) of hydroxylation (Figure S14), In the same way to in vitro selectivity (Fig. S4, α >99%, (S)-92%ee). 100 ns MD simulations of α-hydroxy myristic acid bound CYP152N1 were performed in the same way to myristic acid bound form.

Acknowledgements

This work was supported, in part, by Grants-in-Aid-for Scientific Research (B) to Y. W. (17H03087) and Grants-in-Aid-for Scientific Research on Innovative Areas “Precise Formation of Catalyst Having a Specified Field for Use in Extremely Difficult Substrate Conversion Reactions” to O. S. (15H05806). from the Ministry of Education, Culture, Sports, Science and Technology (Japan), and Grant-in-Aid for JSPS Research Fellow to H. O. (16J02846). from Japan Society for the Promotion of Science (Japan). We thank Dr. Go Ueno, Dr. Hironori Murakami and Dr. Yuki Nakamura for assistance with the data collection at SPring-8. We also thank Prof. David R. Nelson for classification of CYP152 family enzymes.

Notes and references

The atomic coordinates and structure factors (codes **5YHJ**) have been deposited in the Protein Data Bank, Research Collaboratory for Structural Bioinformatics, Rutgers University, New Brunswick, NJ (http://www.rcsb.org/).

The abbreviations used are:

CYP or P450	Cytochrome P450
CYP152s	Cytochrome P450 152 family enzymes (Fatty acid peroxygenases, EC 1. 11. 2. 4)
CYP152N1	Cytochrome P450 isolated from *Exiguobacterium* sp. AT1b ($P450_{Ex\alpha}$)
CYP152A1	Cytochrome P450 isolated from *Bacillus subtilis* IFO14144 ($P450_{BS\beta}$)
CYP152A2	Cytochrome P450 isolated from *Clostridium acetobutylicum* ATCC824 ($P450_{Cla}$)
CYP152A8	Cytochrome P450 isolated from *Alicyclobacillus acidocaldarius* LAA1 (CYP-Aa162)
CYP152B1	Cytochrome P450 isolated from *Sphingomonas paucimobilis* EY2395 ($P450_{SP\alpha}$)
CYP152L1	Cytochrome P450 isolated from *Jeotgalicoccus* sp. 8456 ($OleT_{JE}$)
CYP152L2	Cytochrome P450 isolated from *Staphylococcus massiliensis* S46 (CYP-Sm46)
CYP152P1	Cytochrome P450 isolated from *Methylobacterium populi* sp. nov. (BJ001 ^{T} =ATCC BAA-705 ^{T} =NCIMB 13946 ^{T})[57] (CYP-MP)
C_{16}	Palmitic acid (Hexadecanoic acid)
C_{14}	Myristic acid (Tetradecanoic acid)
C_{13}	Tridecanoic acid
C_{12}	Laulic acid (Dodecanoic acid)
C_{14}α-OH	α-Hydroxymyristic acid
C_{14}β-OH	β-Hydroxymyristic acid
C_{14}α=O	α-Ketomyristic acid (α-Oxomyristic acid)
C_{13}α-OH	α-Hydroxytridecanoic acid

1. M. Sono, M. P. Roach, E. D. Coulter and J. H. Dawson, *Chem Rev*, 1996, **96**, 2841-2888.
2. J. B. van Beilen, W. A. Duetz, A. Schmid and B. Witholt, *Trends Biotechnol*, 2003, **21**, 170-177.
3. B. Holmes, R. J. Owen, A. Evans, H. Malnick and W. R. Willcox, *International Journal of Systematic Bacteriology*, 1977, **27**, 133-146.
4. E. Yabuuchi, I. Yano, H. Oyaizu, Y. Hashimoto, T. Ezaki and H. Yamamoto, *Microbiology and Immunology*, 1990, **34**, 99-119.
5. I. Matsunaga, M. Yamada, E. Kusunose, Y. Nishiuchi, I. Yano and K. Ichihara, *FEBS Lett*, 1996, **386**, 252-254.
6. I. Matsunaga, T. Sumimoto, A. Ueda, E. Kusunose and K. Ichihara, *Lipids*, 2000, **35**, 365-371.
7. I. Matsunaga, M. Yamada, E. Kusunose, T. Miki and K. Ichihara, *J Biochem*, 1998, **124**, 105-110.
8. T. Fujishiro, O. Shoji, S. Nagano, H. Sugimoto, Y. Shiro and Y. Watanabe, *J Biol Chem*, 2011, **286**, 29941-29950.
9. F. Kunst, N. Ogasawara, I. Moszer, A. M. Albertini, G. Alloni, V. Azevedo, M. G. Bertero, P. Bessieres, A. Bolotin, S. Borchert, R. Borriss, L. Boursier, A. Brans, M. Braun, S. C. Brignell, S. Bron, S. Brouillet, C. V. Bruschi, B. Caldwell, V. Capuano, N. M. Carter, S. K. Choi, J. J. Cordani, I. F. Connerton, N. J. Cummings, R. A. Daniel, F. Denziot, K. M. Devine, A. Dusterhoft, S. D. Ehrlich, P. T. Emmerson, K. D. Entian, J. Errington, C. Fabret, E. Ferrari, D. Foulger, C. Fritz, M. Fujita, Y. Fujita, S. Fuma, A. Galizzi, N. Galleron, S. Y. Ghim, P. Glaser, A. Goffeau, E. J. Golightly, G. Grandi, G. Guiseppi, B. J. Guy, K. Haga, J. Haiech, C. R. Harwood, A. Henaut, H. Hilbert, S. Holsappel, S. Hosono, M. F. Hullo, M. Itaya, L. Jones, B. Joris, D. Karamata, Y. Kasahara, M. Klaerr-Blanchard, C. Klein, Y. Kobayashi, P. Koetter, G. Koningstein, S. Krogh, M. Kumano, K. Kurita, A. Lapidus, S. Lardinois, J. Lauber, V. Lazarevic, S. M. Lee, A. Levine, H. Liu, S. Masuda, C. Mauel, C. Medigue, N. Medina, R. P.

Mellado, M. Mizuno, D. Moestl, S. Nakai, M. Noback, D. Noone, M. O'Reilly, K. Ogawa, A. Ogiwara, B. Oudega, S. H. Park, V. Parro, T. M. Pohl, D. Portelle, S. Porwollik, A. M. Prescott, E. Presecan, P. Pujic, B. Purnelle, G. Rapoport, M. Rey, S. Reynolds, M. Rieger, C. Rivolta, E. Rocha, B. Roche, M. Rose, Y. Sadaie, T. Sato, E. Scanlan, S. Schleich, R. Schroeter, F. Scoffone, J. Sekiguchi, A. Sekowska, S. J. Seror, P. Serror, B. S. Shin, B. Soldo, A. Sorokin, E. Tacconi, T. Takagi, H. Takahashi, K. Takemaru, M. Takeuchi, A. Tamakoshi, T. Tanaka, P. Terpstra, A. Togoni, V. Tosato, S. Uchiyama, M. Vandebol, F. Vannier, A. Vassarotti, A. Viari, R. Wambutt, H. Wedler, T. Weitzenegger, P. Winters, A. Wipat, H. Yamamoto, K. Yamane, K. Yasumoto, K. Yata, K. Yoshida, H. F. Yoshikawa, E. Zumstein, H. Yoshikawa and A. Danchin, *Nature*, 1997, **390**, 249-256.

10. J. Nolling, G. Breton, M. V. Omelchenko, K. S. Makarova, Q. Zeng, R. Gibson, H. M. Lee, J. Dubois, D. Qiu, J. Hitti, Y. I. Wolf, R. L. Tatusov, F. Sabathe, L. Doucette-Stamm, P. Soucaille, M. J. Daly, G. N. Bennett, E. V. Koonin and D. R. Smith, *J Bacteriol*, 2001, **183**, 4823-4838.
11. I. Matsunaga, A. Ueda, N. Fujiwara, T. Sumimoto and K. Ichihara, *Lipids*, 1999, **34**, 841-846.
12. M. Girhard, S. Schuster, M. Dietrich, P. Durre and V. B. Urlacher, *Biochem Biophys Res Commun*, 2007, **362**, 114-119.
13. I. Matsunaga, A. Ueda, T. Sumimoto, K. Ichihara, M. Ayata and H. Ogura, *Arch Biochem Biophys*, 2001, **394**, 45-53.
14. D. S. Lee, A. Yamada, H. Sugimoto, I. Matsunaga, H. Ogura, K. Ichihara, S. Adachi, S. Y. Park and Y. Shiro, *J Biol Chem*, 2003, **278**, 9761-9767.
15. R. Ramanan, K. D. Dubey, B. Wang, D. Mandal and S. Shaik, *J Am Chem Soc*, 2016, **138**, 6786-6797.
16. H. Onoda, O. Shoji and Y. Watanabe, *Dalton transactions (Cambridge, England : 2003)*, 2015, **44**, 15316-15323.
17. M. A. Rude, T. S. Baron, S. Brubaker, M. Alibhai, S. B. Del Cardayre and A. Schirmer, *Appl Environ Microbiol*, 2011, **77**, 1718-1727.
18. J. Belcher, K. J. McLean, S. Matthews, L. S. Woodward, K. Fisher, S. E. Rigby, D. R. Nelson, D. Potts, M. T. Baynham, D. A. Parker, D. Leys and A. W. Munro, *J Biol Chem*, 2014, **289**, 6535-6550.
19. J. L. Grant, C. H. Hsieh and T. M. Makris, *J Am Chem Soc*, 2015, **137**, 4940-4943.
20. C. H. Hsieh, X. Huang, J. A. Amaya, C. D. Rutland, C. L. Keys, J. T. Groves, R. N. Austin and T. M. Makris, *Biochemistry*, 2017, **56**, 3347-3357.
21. J. L. Grant, M. E. Mitchell and T. M. Makris, *Proc Natl Acad Sci U S A*, 2016, **113**, 10049-10054.
22. A. Dennig, M. Kuhn, S. Tassoti, A. Thiessenhusen, S. Gilch, T. Bulter, T. Haas, M. Hall and K. Faber, *Angew Chem Int Ed Engl*, 2015, **54**, 8819-8822.
23. J. A. Amaya, C. D. Rutland and T. M. Makris, *J Inorg Biochem*, 2016, **158**, 11-16.
24. H. Xu, L. Ning, W. Yang, B. Fang, C. Wang, Y. Wang, J. Xu, S. Collin, F. Laeuffer, L. Fourage and S. Li, *Biotechnol Biofuels*, 2017, **10**, 208.
25. T. A. Vishnivetskaya, S. Lucas, A. Copeland, A. Lapidus, T. Glavina del Rio, E. Dalin, H. Tice, D. C. Bruce, L. A. Goodwin, S. Pitluck, E. Saunders, T. Brettin, C. Detter, C. Han, F. Larimer, M. L. Land, L. J. Hauser, N. C. Kyrpides, G. Ovchinnikova, S. Kathariou, R. F. Ramaley, D. F. Rodrigues, C. Hendrix, P. Richardson and J. M. Tiedje, *J Bacteriol*, 2011, **193**, 2880-2881.
26. A. Lopalco, G. Dalwadi, S. Niu, R. L. Schowen, J. Douglas and V. J. Stella, *Journal of pharmaceutical sciences*, 2016, **105**, 705-713.
27. A. Lopalco and V. J. Stella, *Journal of pharmaceutical sciences*, 2016, **105**, 2879-2885.
28. C. A. Bunton, *Nature*, 1949, **163**, 444-444.
29. E. Melzer and H. L. Schmidt, *Biochem J*, 1988, **252**, 913-915.
30. A. Lopalco, J. Douglas, N. Denora and V. J. Stella, *Journal of pharmaceutical sciences*, 2016, **105**, 664-672.
31. T. L. Poulos, B. C. Finzel, I. C. Gunsalus, G. C. Wagner and J. Kraut, *J Biol Chem*, 1985, **260**, 16122-16130.
32. K. G. Ravichandran, S. S. Boddupalli, C. A. Hasemann, J. A. Peterson and J. Deisenhofer, *Science*, 1993, **261**, 731-736.
33. A. S. Faponle, M. G. Quesne and S. P. de Visser, *Chemistry*, 2016, **22**, 5478-5483.
34. E. A. Berry and B. L. Trumpower, *Analytical Biochemistry*, 1987, **161**, 1-15.
35. K. G. Paul, H. Theorell and A. Akeson, *Acta Chemica Scandinavica*, 1953, **7**, 1284-1287.
36. Z. Otwinowski, D. Borek, W. Majewski and W. Minor, *Acta Crystallogr A*, 2003, **59**, 228-234.
37. A. Vagin and A. Teplyakov, *Journal of Applied Crystallography*, 1997, **30**, 1022-1025.
38. G. N. Murshudov, A. A. Vagin and E. J. Dodson, *Acta Crystallogr D Biol Crystallogr*, 1997, **53**, 240-255.
39. P. V. Afonine, R. W. Grosse-Kunstleve, N. Echols, J. J. Headd, N. W. Moriarty, M. Mustyakimov, T. C. Terwilliger, A. Urzhumtsev, P. H. Zwart and P. D. Adams, *Acta Crystallogr D Biol Crystallogr*, 2012, **68**, 352-367.
40. P. Emsley and K. Cowtan, *Acta Crystallogr D Biol Crystallogr*, 2004, **60**, 2126-2132.
41. M. D. Winn, M. N. Isupov and G. N. Murshudov, *Acta Crystallographica Section D-Biological Crystallography*, 2001, **57**, 122-133.
42. S. B. Michael Bergdorf, Charles A. Rendleman, and David E. Shaw, *D. E. Shaw Research Technical Report DESRES/TR--2016-01*, 2016.
43. I. Schlichting, J. Berendzen, K. Chu, A. M. Stock, S. A. Maves, D. E. Benson, B. M. Sweet, D. Ringe, G. A. Petsko and S. G. Sligar, *Science*, 2000, **287**, 1615-1622.
44. K. L. Stone, R. K. Behan and M. T. Green, *Proc Natl Acad Sci U S A*, 2005, **102**, 16563-16565.
45. H. Li, A. D. Robertson and J. H. Jensen, *Proteins*, 2005, **61**, 704-721.
46. D. C. Bas, D. M. Rogers and J. H. Jensen, *Proteins*, 2008, **73**, 765-783.
47. W. L. Jorgensen, J. Chandrasekhar, J. D. Madura, R. W. Impey and M. L. Klein, *The Journal of Chemical Physics*, 1983, **79**, 926-935.
48. I. T. Arkin, H. Xu, M. O. Jensen, E. Arbely, E. R. Bennett, K. J. Bowers, E. Chow, R. O. Dror, M. P. Eastwood, R. Flitman-Tene, B. A. Gregersen, J. L. Klepeis, I. Kolossvary, Y. Shan and D. E. Shaw, *Science*, 2007, **317**, 799-803.
49. K. Shahrokh, A. Orendt, G. S. Yost and T. E. Cheatham, 3rd, *J Comput Chem*, 2012, **33**, 119-133.
50. J. L. Banks, H. S. Beard, Y. Cao, A. E. Cho, W. Damm, R. Farid, A. K. Felts, T. A. Halgren, D. T. Mainz, J. R. Maple, R. Murphy, D. M. Philipp, M. P. Repasky, L. Y. Zhang, B. J.

Berne, R. A. Friesner, E. Gallicchio and R. M. Levy, *J Comput Chem*, 2005, **26**, 1752-1780.
51. J.-P. Ryckaert, G. Ciccotti and H. J. C. Berendsen, *Journal of Computational Physics*, 1977, **23**, 327-341.
52. S. Nosé, *Molecular Physics*, 1984, **52**, 255-268.
53. W. G. Hoover, *Phys Rev A Gen Phys*, 1985, **31**, 1695-1697.
54. G. J. Martyna, M. L. Klein and M. Tuckerman, *The Journal of Chemical Physics*, 1992, **97**, 2635-2643.
55. G. J. Martyna, M. E. Tuckerman, D. J. Tobias and M. L. Klein, *Molecular Physics*, 1996, **87**, 1117-1157.
56. M. Tuckerman, B. J. Berne and G. J. Martyna, *The Journal of Chemical Physics*, 1992, **97**, 1990-2001.
57. B. Van Aken, C. M. Peres, S. L. Doty, J. M. Yoon and J. L. Schnoor, *International journal of systematic and evolutionary microbiology*, 2004, **54**, 1191-1196.